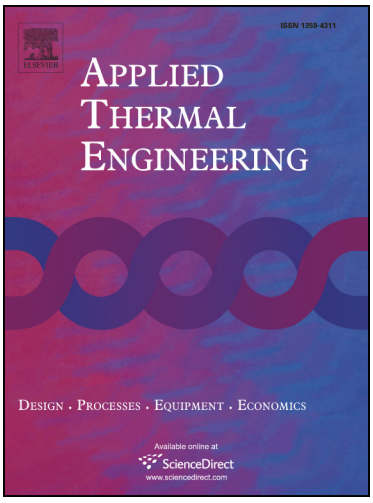

Electricity demand flexibility performance of a sorption-assisted water storage on building heating

Yongbao Chen, Aditya Desai, Ferdinand Schmidt, Peng Xu

PII: S1359-4311(18)36697-3
DOI: https://doi.org/10.1016/j.applthermaleng.2019.04.080
Reference: ATE 13670

To appear in: *Applied Thermal Engineering*

Received Date: 31 October 2018
Revised Date: 8 April 2019
Accepted Date: 18 April 2019

Please cite this article as: Y. Chen, A. Desai, F. Schmidt, P. Xu, Electricity demand flexibility performance of a sorption-assisted water storage on building heating, *Applied Thermal Engineering* (2019), doi: https://doi.org/10.1016/j.applthermaleng.2019.04.080

Electricity demand flexibility performance of a sorption-assisted water storage on building heating

Yongbao Chen[1,2], Aditya Desai[2], Ferdinand Schmidt[2], and Peng Xu[1*]

[1]*School of Mechanical and Energy Engineering, Tongji University, Shanghai, 201804, China*

[2]*Institute of Fluid Machinery, Karlsruhe Institute of Technology, Karlsruhe, 76131, Germany*

Abstract: The energy performance and energy flexibility potential of a sorption-assisted water storage (SAWS) for a medium-scale residential building with eight apartments under the climatic condition of Potsdam, Germany were investigated. The SAWS system consists of a stratified water storage coupled to an adsorption heat pump (AHP). The driving heat source for the AHP was modeled as an ideal heater, which can be interpreted as an electric heater to serve as an off-peak storage heating system. Five representative partial heating loads of a building were investigated. Recharging situations of 2 h, 4 h, and 8 h with an interval of 2 h heater switching off were considered. Transient simulation results show that the 2 h heater switch off is feasible and does not significantly reduce the occupants' thermal comfort in the four low heating load cases. However, for the highest heating load case, the load cannot be completely met. An average heating coefficient of performance of 1.33 for all the five load cases is achieved. Additionally, under the simple control scheme considered here, this SAWS system achieves high electricity flexibility by controlling the heater switch on and off schedule for a demand response program.

Key words: Adsorption heat pump; Demand response; Energy flexibility; Heating performance; Stratified storage water tank

Nomenclature

c_p	Specific heat capacity	*zones*	Number of temperature zones (extraction)
H_{cooler}	The ratio of cooler flow inlet and tank height	ΔT	Temperature differential (°C)
H_{heater}	The ratio of heater flow inlet and tank height	ρ	Density (kg/m^3)
M_{cooler}	Mass flow through cooler side (kg/s)		
M_{cond}	Mass flow through condenser side (kg/s)	**Abbreviations**	
M_{evap}	Mass flow through evaporator side (kg/s)	*AHP*	Adsorption heat pump
M_{rad}	Mass flow through building heating system ($M_{rad} = M_{cond} + M_{cooler}$) (kg/s)	*DR*	Demand response
M_{sys}	System mass flow from storage tank to adsorber (kg/s)	*F*	Energy flexibility
$q_{eff,ref}$	Unit effective storage density of normal	*HTHP*	High-temperature vapor

* Corresponding author: Prof. Peng Xu; phone number: +86 13601971494;
email address: xupeng@tongji.edu.cn

	system (kWh/m^3)		compression heat pump
$q_{eff,SAWS}$	Unit effective storage density of SAWS system (kWh/m^3)	*P*	Power (kW)
T_{diff}	Temperature switching setting between two extraction rings (°C)	*SSWT*	Stratified storage water tank
T_{return}	Return water temperature from building heating system (°C)	*SAWS*	Sorption-assisted water storage
T_{supply}	Supply water temperature to building heating system (°C)	*TES*	Thermal energy storage

1 Introduction

The progress in solar and wind power generation technologies in recent years has opened up a transformation path for energy systems along which the share of variable renewable energy (VRE) in the power grids is increasing rapidly, while the learning curves of these technologies are quickly decreasing the generation costs [1, 2]. Integration of this increasing share of VRE into energy systems is a major challenge for the next decades. Renewable power curtailment due to insufficient grid capacity is already becoming a significant problem in some regions, e.g., in northern China [3] and in Germany [4]. Besides grid extension, electricity storage is one option to be developed, as well as conversion of power to heat [5, 6] and increasing power demand flexibility through demand response (DR) measures [7].

For the building sector in heating-dominated climatic zones of the world, the two key challenges of energy transformation are heating demand reduction through improvement of building skins and de-carbonization of heating systems [8]. In most energy transformation scenarios, electric heat pumps with vapor compression cycle come out as the dominant heating technology for the target system. Several studies have analyzed the effects of increased utilization of heat pumps with thermal storage on grid integration of VRE. Hedegaard et al. [9] found in their simulation study for single-family houses in Denmark that combining heat pumps with “passive heat storage” in the building mass by allowing temperature variations within the comfort range provides a significant and cost-effective way of improving grid integration of wind power. Additional integration of water storage tanks was found to provide additional flexibility[9]. A more recent review by Fischer and Madani [13] reported similar results from a range of different studies and points out that heat pump/thermal storage systems have the additional benefit of reducing the need for backup power.

Typical vapor compression heat pumps for buildings can only use a limited temperature range of a hot water storage. The energy density of the storage can be increased significantly if the temperature range of the storage cycle can be extended. This requires adapted heat pump cycles like transcritical or cascading cycles, which we do not analyze any further in this contribution. Inevitably, heating a hot water storage to temperatures higher than required for heating the building will require a higher temperature lift of the compression heat pump and thus lower its efficiency (compared to direct heating without storage). The idea of the sorption-assisted water storage (SAWS) is to utilize an adsorption heat pump (AHP) to achieve an

efficiency gain during the discharging of the storage and thus to compensate the efficiency loss during the charging phase.

Research on AHPs and chillers has aimed at improving the coefficient of performance (COP) and specific power output. In order to achieve this, one key research area is on new materials for AHPs. Adsorbents, which have been tailored for specific applications, particularly dealuminated zeolites [14], substituted aluminophosphates, composite "salt in porous host matrices," and metal-organic frameworks[15, 16]. The direct crystallization of SAPO-34 has also been studied by Bonaccorsi et al. [17], where the use of graphite foams as substrate showed a higher thermal conductivity compared to aluminum foams. Rivero-Pacho et al. [18] studied adsorption modules with three alternative activated carbon composites using ammonia as working fluid.

Another key research direction in this area has been the improvement of the heat and mass transfer in adsorber heat exchangers. Different methods for applying the adsorbent to the metal surface of the heat exchanger, including various coating technologies and their characterization, have been discussed in[19, 20]. One promising approach is the direct in situ crystallization method described by Bauer et al. [21]. A scaled eZea module, from Fahrenheit GmbH (formerly SorTech AG), where the same coating method is applied to a fin-and-tube heat exchanger, was used as the AHP in the current work, as a dynamic model for this type was readily available. This approach has been further investigated by Wittstadt et al. [22, 23] in a novel adsorption module, which uses a composite of sintered aluminum fibers with an in situ crystallized coating of silico-aluminophosphate (SAPO-34). A heating COP of 1.4 without heat recovery and a volume specific power of 320 W/L was demonstrated using this adsorption module.

Apart from the development of improving energy performance, energy flexibility is also one aspect that should be considered in the future. Buildings account for a large proportion of electrical demand, particularly for heating, ventilation, and air conditioning (HVAC) systems. Using well-designed thermal storage HVAC systems can shift electric demands from peak load time to peak-valley time and provide energy flexibility for building load management and DR programs. Energy system with flexibility is a promising way of balancing the electricity supply and demand side in the electricity market recently, especially that a large proportion of renewable energy, such as solar energy and wind power, is pouring into the grid [24]. Coupling the electricity and heat with energy storage was introduced in many studies. Felten and Weber [25] proposed a coupled building and heat pump with a storage tank system to investigate energy flexibility. A power-to-heat system has been studied as a flexibility resource in [26].

While systems with AHP often also contain a hot water storage, that storage is normally not being used as a driving heat source for the AHP. For adsorption chillers (ACH), however, a configuration in which a hot water storage driving the ACH is quite common, e.g. in combined heating, cooling and power (CHCP) systems [27]. In our SAWS system, the hot water tank is being operated as a stratified storage for a thermodynamically improved coupling to the adsorption cycle, as detailed by Schwamberger and Schmidt[28] . The stratified storage water tank (SSWT) features multiple water inlets/outlets (rings) at different heights of the tank so that the released heat from adsorption half cycle can be stored at different temperature levels. One objective of this study is to improve the SAWS energy efficiency on a real building application

by optimizing the system parameters, which include system mass flow, ring temperature differential, zone number, position height of heater and cooler, and condenser and cooler mass flow. Another objective is to investigate the energy flexibility potential of this SAWS system in a DR context. The remainder of this paper is organized as follows. In Section 2, we describe the SAWS system. In Section 3, the definition of energy flexibility and COP are presented. In Section 4, we introduce the SAWS system model. In Section 5, the simulation scenarios are described. In Section 6, we provide the corresponding results and discussions. In Section 7, we present our main conclusions.

2 SAWS system description

The SAWS system consisting of a stratified hot water storage coupled to an AHP is considered here for larger buildings (multi-family residential as well as non-residential buildings). Initial results on the storage discharging behavior of such a system were reported by Schwamberger and Schmidt [28] and by Li et al. [29]. The SAWS system provides two key benefits compared to a standard water storage tank coupled to a vapor compression heat pump. First, the heat stored in the SAWS tank at a temperature higher than currently required by the heating system is utilized via the AHP, thus adding ambient heat to the useful heat and increasing system efficiency. When the SAWS tank is charged by a high-temperature vapor compression heat pump (HTHP), the usable temperature range of the sensible storage is larger than when using a standard heat pump and tank, which in combination with the sorption effect can lead to a considerable increase in the effective energy density of the storage. For example, if the minimal usable heating temperature is 30 °C and the standard heat pump can charge the storage up to 60 °C in a normal system, the usable temperature spread is 30 °C and the effective energy density per volume of stored water is

$$q_{eff,ref} = c_p \cdot \rho \cdot \Delta T_{ref} \approx 35 \frac{\text{kWh}}{\text{m}^3} \tag{1}$$

For SAWS with an assumed maximum HTHP charging temperature of 100 °C and a 1.2 average COP of the AHP during storage discharge, the effective storage density of SAWS is

$$q_{eff,SAWS} = c_p \cdot \rho \cdot \Delta T_{SAWS} \cdot COP_{discharge} \approx 84 \frac{\text{kWh}}{\text{m}^3} \tag{2}$$

In this example, the effective storage density of SAWS is higher by a factor of 2.4, which in many use cases means a similar increase in the installable storage capacity, considering the usual space limitations of existing boiler rooms in the building stock. The storage charging COP of the HTHP will of course be considerably lower than that of the standard heat pump, but the discharging COP of SAWS narrows this performance gap. The second of the abovementioned SAWS benefits is that the "sorption assist" works with any heat source used to charge the storage. If, for example, a gas burner is used as a backup/peak load heater with the HTHP, the system can work as a gas heat pump and make use of the ambient heat source independently of its operating mode. In this initial study regarding the demand flexibility provided by the SAWS system, we consider only an ideal heater in our model, which could later be replaced by an HTHP model or a

hybrid heating system model. Here, a simple heating rod (electrical resistance heater) can be used as a heater.

To improve the COP of SAWS, the Institute of Fluid Machinery of Karlsruhe Institute of Technology has been researching the heat recovery of AHP systems, with a particular focus on the Stratisorp system in which the AHP is coupled to an SSWT for internal heat recovery between the adsorption and desorption half cycles [28, 30, 31]. As commonly known, the AHP operates in periodic cycles, which include adsorption and desorption half cycles. In the adsorption half cycle, the refrigerant (adsorbate) vaporizes in the evaporator adsorbing heat from the low-temperature heat source. Thus, the heat pumping effect from the low-temperature heat source to the temperature for usable heat is achieved. The adsorber is then regenerated by connecting it to an external heat source at a higher temperature. In the desorption half cycle, adsorbate vapor is driven out from the adsorbent and is condensed in the condenser, where more usable heat is released. The SSWT in the Stratisorp system allows storing the heat released during the adsorption half cycle, which can reduce the external heat required during the desorption half cycle.

In this study, this system called SAWS is considered. Similar systems have also been studied earlier [28, 29, 32]. A sketch of this proposed system is shown in Fig. 1. The system consists of an AHP module, a stratified storage tank, electricity heater, building module and ground heat source module. The AHP module contains an adsorber and another heat exchanger, which operate alternately as evaporator and condenser, enclosed in a vacuum chamber and an SSWT. The SSWT can be charged using an external heat source (electric heater). Because electricity DR is considered in this study, an electric heater is used as the heat source. However, it can also be replaced by any other energy sources, such as solar energy, industrial waste heat, or a compression heat pump. The SAWS system can provide heating continuously by extracting heat directly from the lower part of the SSWT during the entire cycle. The detailed configuration of SSWT can be seen in Fig. 2. The building heating system thus serves as a cooler for the SSWT. During the desorption half cycle, the condenser of the AHP is also connected to the building heating system. The adsorber of the AHP is connected to the SSWT and is cooled/heated during the adsorption/desorption half cycle, respectively. The AHP extracts heat at a low temperature for the evaporator from the ground using a borehole heat exchanger.

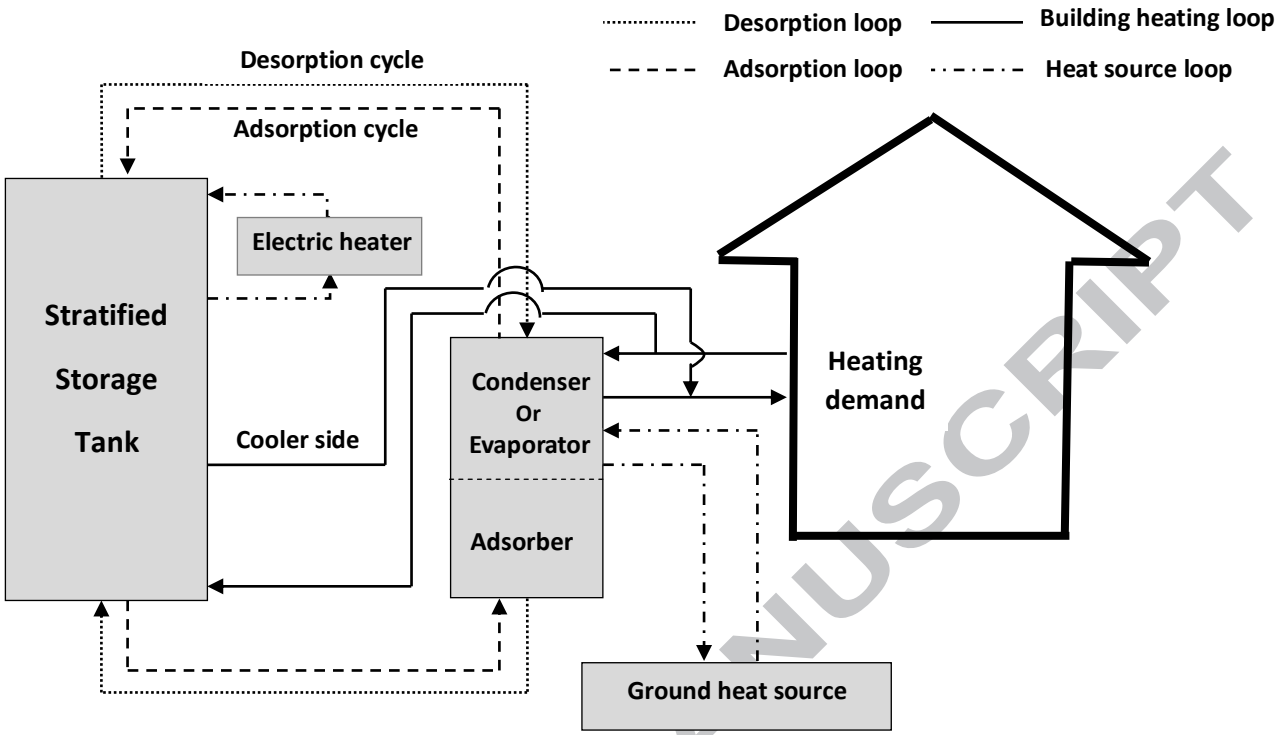

Fig. 1 Sketch of SAWS system for building heating

3 Energy demand flexibility and COP definition

As heat is extracted from the storage tank during the desorption half cycle and part of that heat is recovered by the storage tank during the adsorption half cycle, real-time heating COP is not applicable for AHP, and usually the COP is given as a cycle average. While there are some special conditions existing, one is called stationary cycle that means the amount of stored energy in tank keeps constant at the beginning of each cycle, the other is the heater closed condition so that the stored energy in the tank is used to drive the AHP. Thus, the heating COP of each cycle is proposed and calculated using Eq. 3.

$$\mathrm{COP}_{h,cycle} = \frac{Q_{condenser,cycle} + Q_{cooler,cycle}}{Q_{heater,cycle} - \Delta Q_{tank,cycle}} \tag{3}$$

where $Q_{heater,cycle}$ is the heat from electric heater side of each cycle, $\Delta Q_{tank,cycle}$ is the heat variation of each cycle of the storage tank, $Q_{condenser,cycle}$ and $Q_{cooler,cycle}$ are the heat supply for heating by the condenser and cooler sides of each cycle, respectively. For stationary SAWS cycles, $\Delta Q_{tank,cycle}$ is zero. In the case of electric heater switch off cycles, $Q_{heater,cycle}$ is zero.

In real applications, usually, the dynamic electricity price, DR event triggering, and duration time are difficult to predict in advance. Thus, a common grid peak period, a duration time of DR event (e.g., 2 h), and thermal capacity of the storage tank are considered in this study. Eq. 4 shows the heater switch on and off schedule for one day.

$$Heater = \begin{cases} on & t = 0–8; 10–12; 14–18; 20–24 \\ off & t = 8–10; 12–14; 18–20 \end{cases} \quad (4)$$

The SSWT can be charged using peak-valley or lower price electricity, while discharging during peak electric load or high electricity price time. The SSWT works as a heat buffer so that the SAWS system can provide energy flexibility F (W), which is defined in Eq. 5. The energy flexibility is described in the power system as the ability to cost-effectively and continuously balance electricity supply and demand, while simultaneously maintaining acceptable service quality to connected loads [33]. The common nomenclatures are delayed load, forced load and so on. More information about the definition of energy flexibility can be found in our previous research [34].

$$F(t) = P_{actual}(t) - P_{ref}(t) \quad (5)$$

where P_{actual} is the actual heater power when the heater switch on and off schedule is executed. P_{ref} is the reference heater power when the heater works with no interruption condition. The maximum available (potential) flexibility is equal to the maximum heater power. Normally, during the peak-valley and lower price electricity time, the tank could be forced to fully charge to increase energy consumption, which is characterized as positive flexibility. During the peak load and high price electricity time, the tank stops charging to decrease energy consumption, which means that the flexibility is negative by this time.

4 SAWS system modeling

The SAWS modeling includes the two main parts: AHP and SSWT. The model for the AHP describes the heat and mass transfer in its various parts. The evaporator/condenser is modeled by a single temperature node. On the other hand, the adsorber is discretized in one dimension along the flow direction of the heat transfer fluid (here, water). The vapor transport in and out of the adsorber is described using a linear driving force model. The SSWT is also discretized in one dimension along its height, as illustrated in detail in Fig. 2. The forced convection caused by the water flowing into/from the adsorber, heater, and cooler is modeled as a fractional plug flow, while the natural convection and conduction between neighboring tank nodes are modeled using an amplified thermal conductivity of the water above its natural value. The component and system models are implemented in MATLAB®. A detailed description of the model can be found in the Ph.D. thesis and a conference paper of Schwamberger [30, 35].

The SSWT is fitted with water distribution rings at different heights, which can be used to extract water from the tank or return it back into the tank, as shown in Fig. 2. This system has been investigated in previous experimental studies [29, 31]. The adsorber can be connected to different rings during the cycle, which allows the internal heat recovery of the AHP to be controlled. In the desorption half cycle, the adsorber is heated, i.e., water is extracted from the SSWT, pumped through the adsorber, and reintroduced at a ring lower than the extraction level. This process starts at the bottom of the tank and continues into successively higher rings until the top of the storage tank is reached. The rings for extraction are chosen such that a minimum

temperature differential (T_{diff}) between the water inlet and outlet temperatures is always maintained. This process continues until water is being extracted from the uppermost ring and the temperature difference between the inlet and outlet is less than a critical value ($T_{diff,\ min}$) when the extraction and introduction levels are switched and the adsorption half cycle begins. The operational process for the adsorption half cycle is similar, with water being initially extracted near the top of the tank and then from successively lower rings.

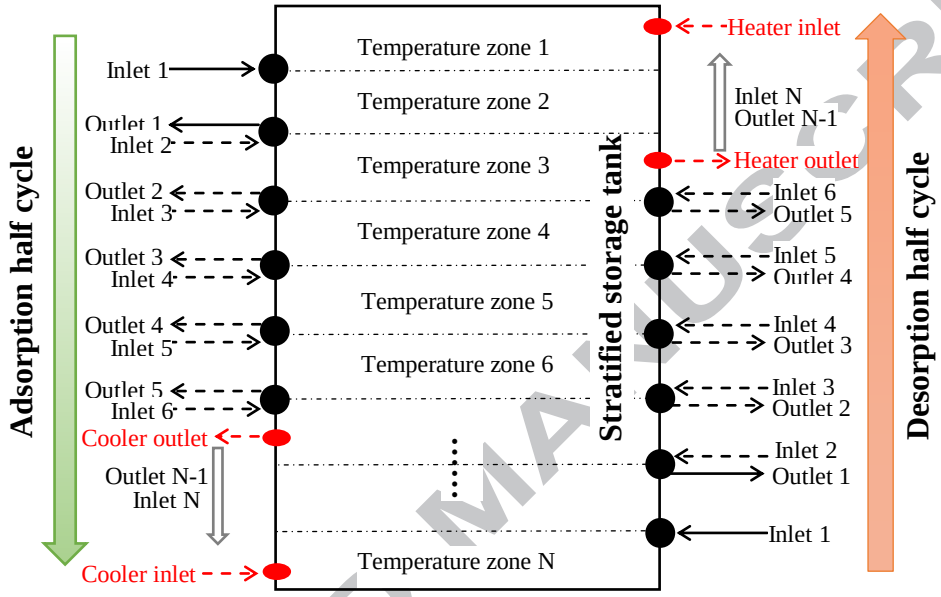

Fig. 2 Operational process sketch of SSWT

In order to meet the heating demand for the building case considered here, a fictitious "scaled" version of the eZea module from Fahrenheit GmbH was used as the AHP. The working pair for the AHP is water/SAPO-34, and the adsorber technology is based on consumptive crystallization of the adsorbent on its support [36]. The volume of the storage tank is 2.25 m^3 according to the results of the energy performance in our previous experiment [29]. To avoid the high cost in pressure vessels, the maximum temperature in the storage and the maximum regeneration temperature was chosen as 100 °C. The undisturbed ground temperature for the building location is 9.54 °C. All the main parameter settings for the simulation are listed in Table 1 in the Appendix.

5 Simulation

5.1 Case building description

The case building is located in Potsdam, Northern Germany, and there are eight apartments in this building. Normally, there is no cooling demand for the whole year. The temperature is below −10 °C in the coldest winter; therefore, a ground heat source is considered. Fig. 3 shows the ambient temperature and air-conditioning heating demand of this building case.

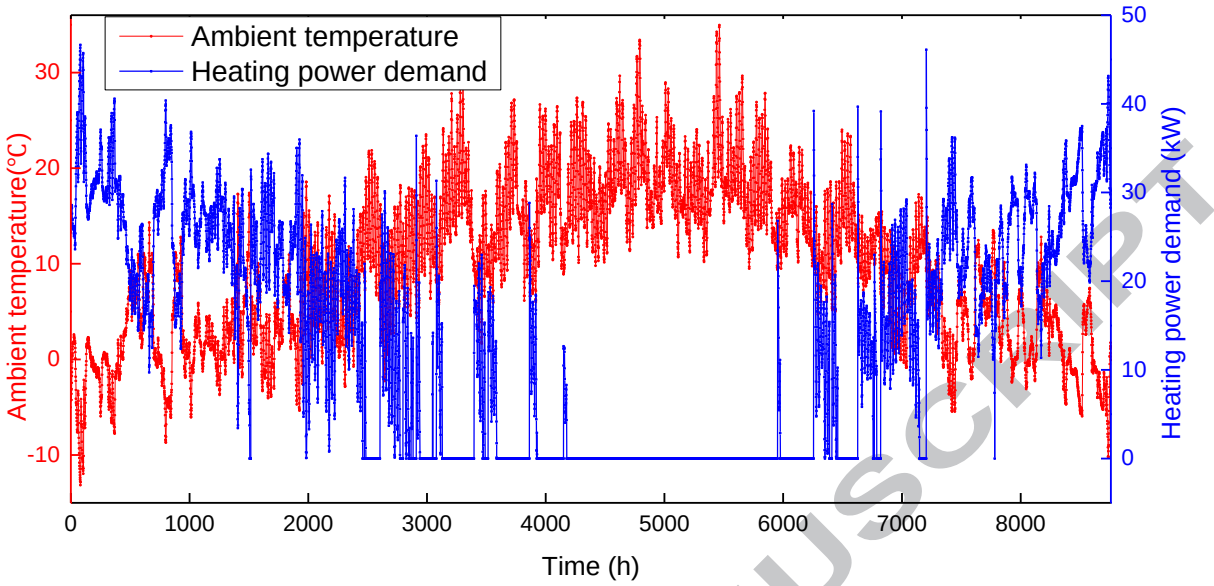

Fig. 3 Ambient temperature and air-conditioning heating demand of building case

The calculation of the energy heating efficiency of thermally driven heat pumps is based on the standard efficiency of modulating condensing boilers according to DIN 4650. It is determined from five representative part-load points, each of which represents one-fifth of the annual heating demand. The average annual gas utilization efficiency can thus be calculated by simply averaging the partial loads at 27%, 44%, 53%, 61%, and 72% of the full load, respectively. In a similar way, the standard energy performance of the AHP is determined by these five part-load outputs corresponding to the related heating demand. Fig. 4 shows the load duration curve and the five related heating demand part loads of this building case. Every area is equivalent, and the numbers on the top of different areas are the average heating demand of each of the five parts. These five average heating demand part loads are 34.5 kW, 29.3 kW, 25.7 kW, 21.2 kW, and 13.0 kW corresponding to relative output ratios of 72%, 61%, 53%, 44%, and 27% of the AHP system, respectively. Hereafter, we designate these five part loads as 72%_P, 61%_P, 53%_P, 44%_P, and 27%_P.

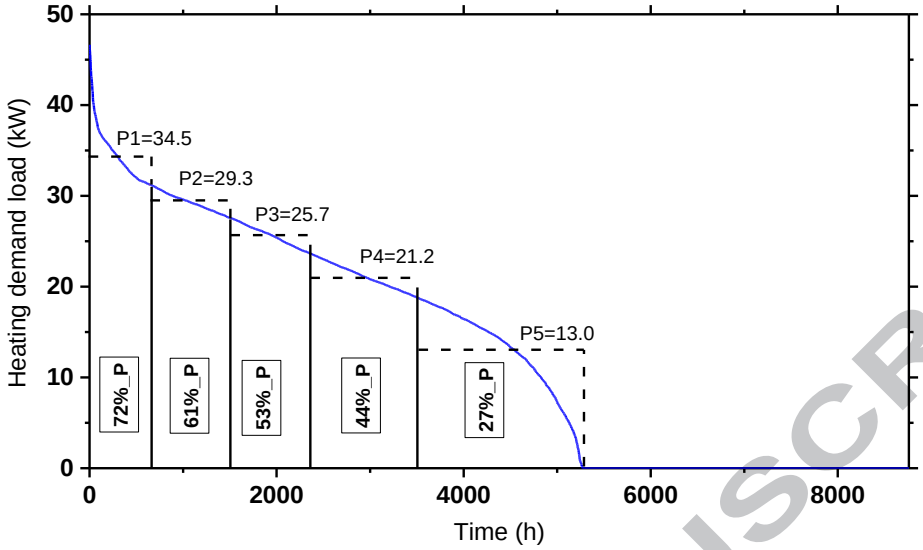

Fig. 4 Five related heating demand part loads of building case

The designed water supply and return temperatures of the AHP system are 45 °C and 35 °C, respectively. The supply and return temperatures of the different power output loads are listed in Table 1. The hourly heating demand and ambient temperature that satisfy the 72%_P situation are shown in Fig. 5. It can be observed that the heating load demand in the night is higher than in daylight.

Table 1 Supply and return temperatures of different part-load outputs

Power output ratio (%)	Supply temperature (°C)	Return temperature (°C)
27	27.1	24.4
44	31.3	26.9
53	33.6	28.2
61	35.4	29.3
72	38.1	30.9
100	45.0	35.0

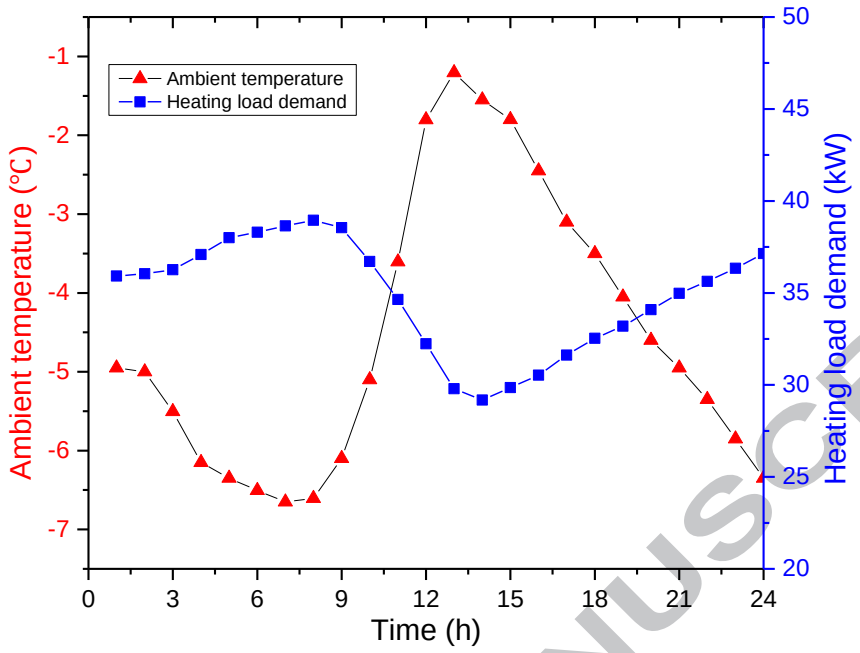

Fig. 5 Heating demand and ambient temperature at 72%_P load case (January 14)

5.2 Simulation scenarios

Table 2 shows the parameter settings for the different parameters optimization scenarios. Table 3 shows the main parameter setting information for different representative loads. More detailed information on the parameter setting is provided in Table 1 of the Appendix. Note that the real building heating demand is fluctuating in one day (see Fig. 5), while we only export enough average heating power from the proposed system as the heating supply for each five part loads (see Fig. 4), which was calculated according to the method in VDI 4650. Actually, it is possible to meet the real-time heating demand by changing M_{cond} and H_{cooler} in the real application.

Table 2 Main parameter setting information for different parameters optimization scenarios

Scenarios	Objective parameter range	Other parameter setting
Scenario 1	M_{sys} (2.0–3.5 kg/s)	M_{sys} = 2.4 kg/s T_{diff} = 5 °C *Zones* = 6 H_{heater} = 0.6 H_{cooler} = 0.4 M_{cond} = 0.6 kg/s T_{return} = 30.9 °C
Scenario 2	T_{diff} (2–8 °C)	
Scenario 3	*Zones* (2–14)	
Scenario 4	H_{heater} (0.5–0.8)	
Scenario 5	H_{cooler} (0.2–0.5)	

Scenario 6	M_{cond} (0.1–1.145)

Table 3 Main parameters setting information for representative loads

Representative load parts	Main parameter setting
72%_P	M_{sys} = 3.0 kg/s T_{diff} = 5 °C M_{cond} = 0.6 kg/s T_{return} = 30.9 °C
61%_P	M_{sys} = 2.1 kg/s T_{diff} = 5 °C M_{cond} = 1.145 kg/s T_{return} = 29.3 °C
53%_P	M_{sys} = 1.7 kg/s T_{diff} = 4 °C M_{cond} = 1.145 kg/s T_{return} = 28.2 °C
44%_P	M_{sys} = 1.3 kg/s T_{diff} = 4 °C M_{cond} = 1.145 kg/s T_{return} = 26.9 °C
27%_P	M_{sys} = 0.7 kg/s T_{diff} = 3 °C M_{cond} = 1.145 kg/s T_{return} = 24.4 °C

6 Results and discussions

6.1 Effects of factors on SAWS energy performance

In this section, we present the investigation of suitable system parameter settings and the energy performance of the case building. The aim is to select some system parameter settings, which are kept constant throughout the subsequent simulations to meet the required load at a high energy performance. In order to investigate the optimal parameter setting in this condition, the 72%_P case is investigated. Noticeably, the electric heater switches off is not considered for all scenarios in this section. The simulation time lasts for 24 h including cycles of up to 150. Avoiding the initial conditional parameter setting in all cases, such as the initial tank temperature, the simulation results are taken from the state when the system is not affected by the initial setting anymore. The main parameter settings in different cases are presented in Table 2. The heating power, heating COP, and T_{supply} shown in the next figures are the average values during

the whole simulation day. As a typical feature of the "Stratisorp" cycle, the *zones*, H_{heater}, and H_{cooler} will be fixed once they are determined.

6.1.1 Scenario 1: M_{sys} effect on heating performance

M_{sys} is the mass flow from the storage tank to the adsorber and return. The effect of M_{sys} on the SAWS heating performance at 72%_P is shown in Fig. 6. It can be observed that as M_{sys} increases, the supply heating power and T_{supply} also increase, while the heating COP decreases. For the 72%_P case, the daily mean demand heating power is 34.5 kW and the supply water temperature T_{supply} is 35.9 °C (refer to Fig. 2 and Table 1).

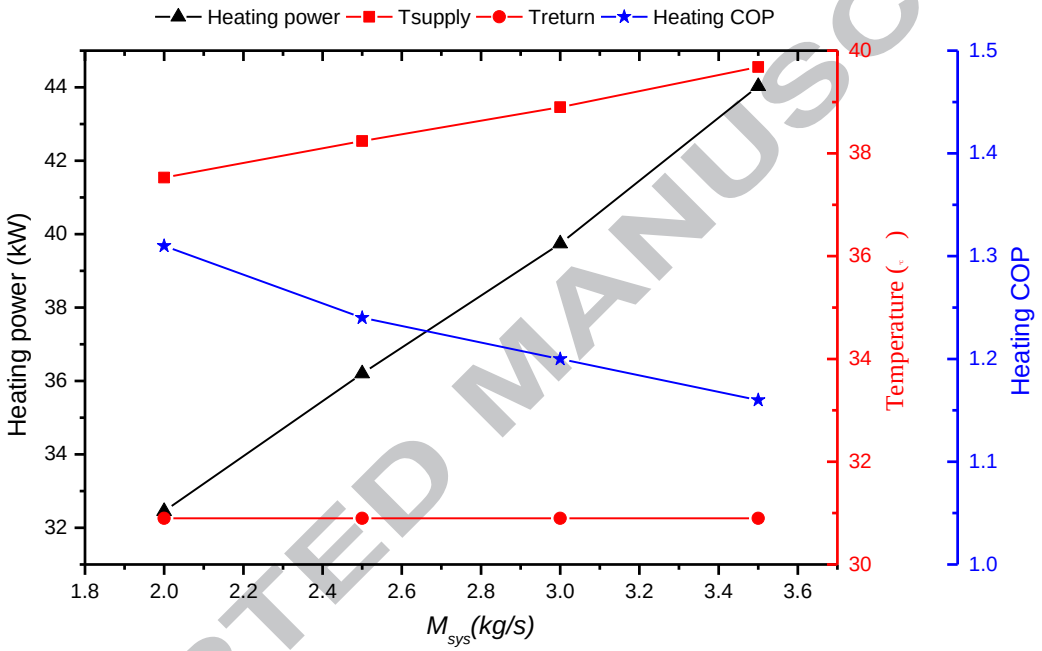

Fig. 6 Effect of M_{sys} on SAWS system heating performance at 72%_P load

6.1.2 Scenario 2: T_{diff} effect on heating performance

T_{diff} is the minimum water temperature difference between the water inlet and outlet of one temperature zone at the time of switching the extraction/introduction height (see Fig. 2). The effect of T_{diff} on heating performance is shown in Fig. 7. It can be observed that as T_{diff} increases, the T_{supply} and heating power increase, while the heating COP decreases. According to the 72%_P conditions, T_{diff} should be higher than 4.0 °C. In addition, when T_{diff} is higher than 4 °C, the curve gradient of heating power and T_{supply} is nearly flat, which denotes that the increase in T_{diff} could only improve the heating power slightly.

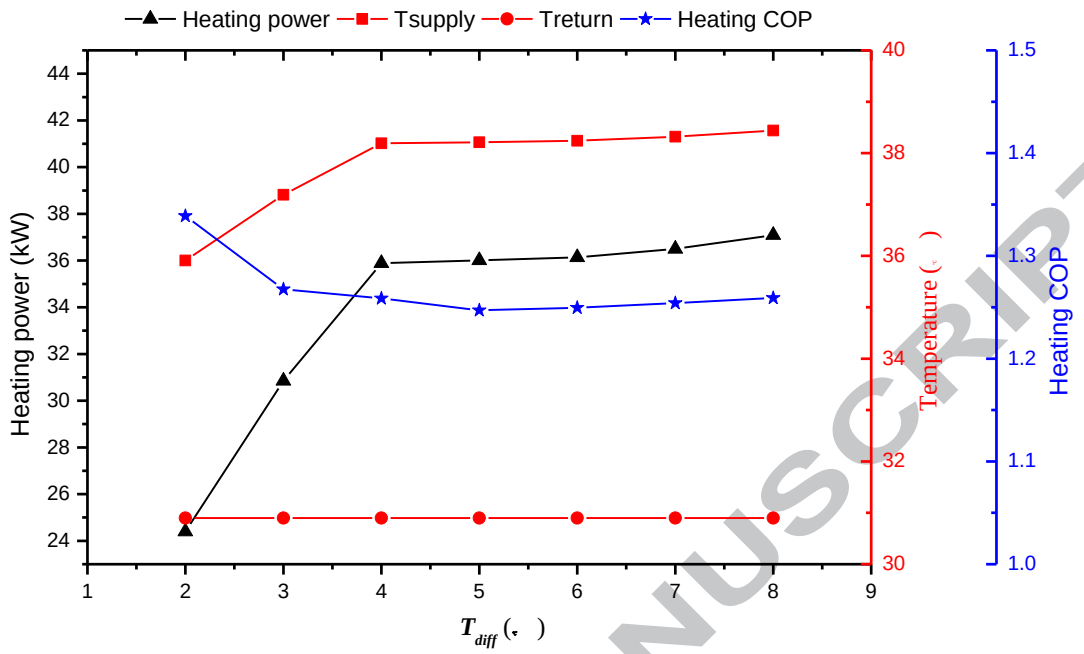

Fig. 7 Effect of T_{diff} on heating performance at 72%_P load

6.1.3 Scenario 3: *zone* effect on heating performance

The effect of the number of zones of SSWT on the heating performance is shown in Fig. 8. It can be observed that as the number of zones increases, the T_{supply} and heating power decrease, while the heating COP increases. The number of zones should be smaller than six to meet the heating demand, while a larger number of zones result in a higher heating COP. In our transient simulation case, when the number of zones is larger than eight, the curve gradient of the heating COP, heating power, and supply temperature are flat, which means that increasing the number of zones can only improve the heating COP slightly. For real applications, the larger the number of zones, the higher the complexity and the cost of the SAWS system. Therefore, less than eight zones should be considered. In this study, the number of zones was set as six for all other cases.

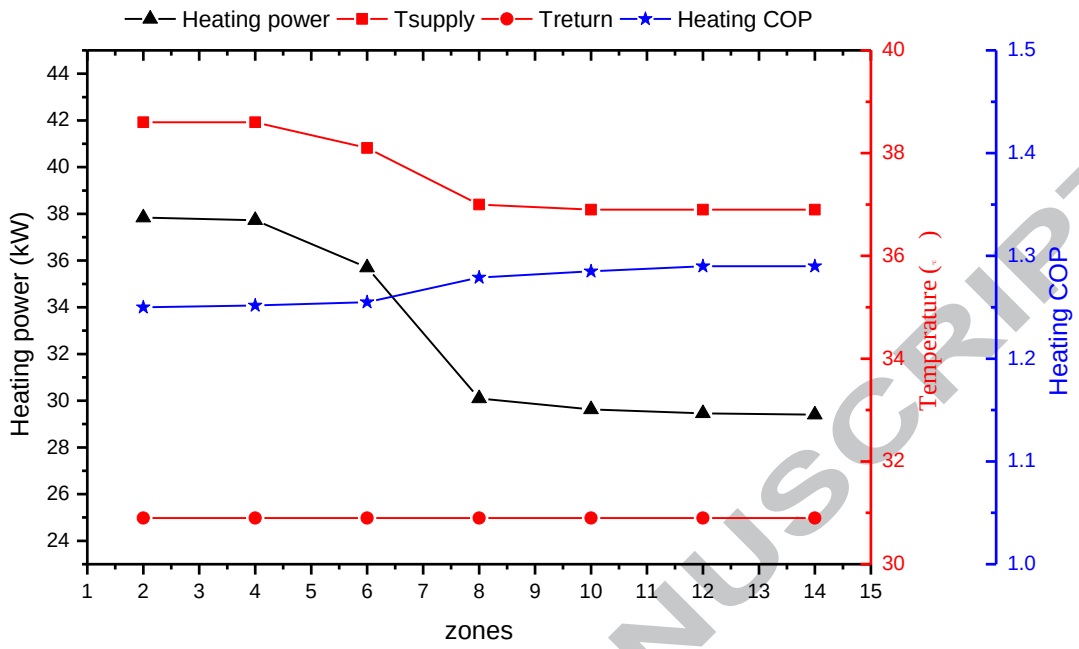

Fig. 8 Effect of number of zones of SSWT on heating performance at 72%_P load

6.1.4 Scenario 4: H_{cooler} and H_{heater} effect on heating performance

H_{cooler} and H_{heater} are the water extraction positions on the SSWT of cooler and electric heater respectively. Here, using the ratio of water extraction height and storage height as the position index, H_{heater} increased from 0.5 to 0.8 (H_{cooler} = 0.4) and H_{cooler} increased from 0.2 to 0.5 (H_{heater} = 0.4). The effect of H_{heater} on heating performance is shown in Fig. 9. It can be observed that when H_{heater} is within the range of 0.65–0.80, as the H_{heater} increases, the gradient of heating COP, heating power, and T_{supply} curves are flat. In the real building case, a lower H_{heater} will sacrifice the heating COP. In this study, a heater extraction height of 60% of the tank height was selected for all succeeding analysis (i.e., H_{heater} is 0.6).

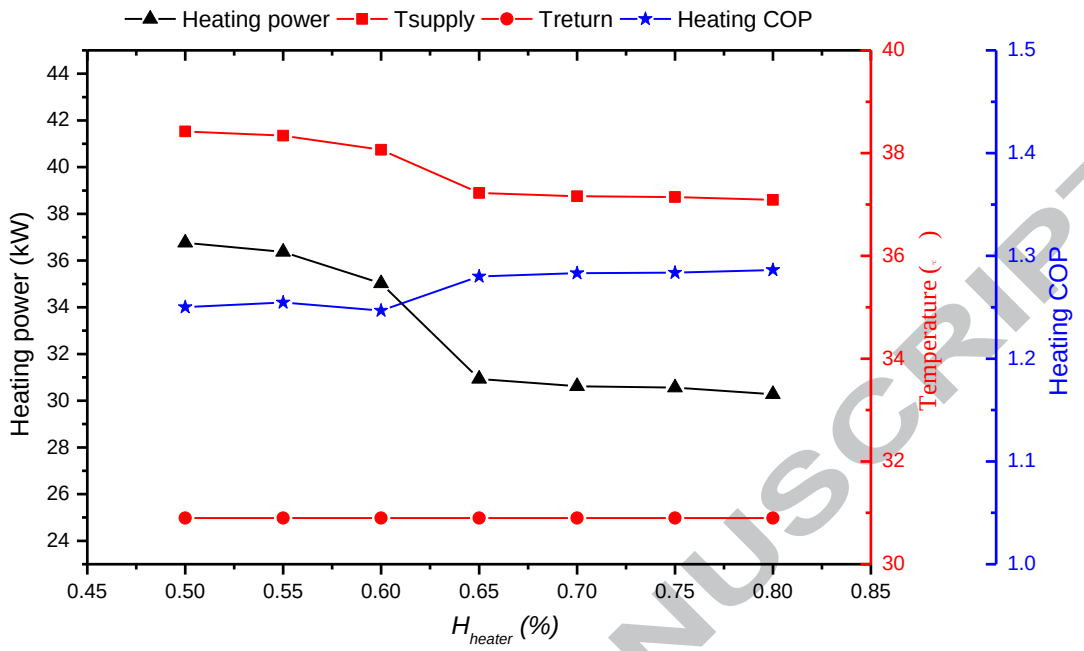

Fig. 9 Effect of H_{heater} of SSWT on heating performance at 72%_P load

At H_{cooler} side, heated water is extracted from the SSWT for heating demand directly. The effect of H_{cooler} on heating performance is shown in Fig. 10. It can be observed that the heating COP is higher at lower H_{cooler}. This is because a lower H_{cooler} will extract less heat from the tank for direct heating, and a large amount of heat in the upper-temperature zones can be used to drive the adsorber for higher energy performance. In this study, a cooler extraction height of 40% of the tank height was selected for all succeeding analysis (i.e., H_{cooler} = 0.4). Although H_{cooler} is fixed during specific cases, it is an interesting open topic if the H_{cooler} is changeable (or unfixed) with multiport valves in real applications. In the unfixed H_{cooler} case, although the heating COP might be decreased, more heat at the top of storage tank can be used directly when there is not enough heat to drive the adsorber, which means that the storage tank can provide a longer heater switch off interval to realize more energy flexibility, while the recharging time would be longer if the heat in tank is exhausted deeply. We can observe from Fig. 14 that there is still a lot of heat at the top of the tank for direct heating.

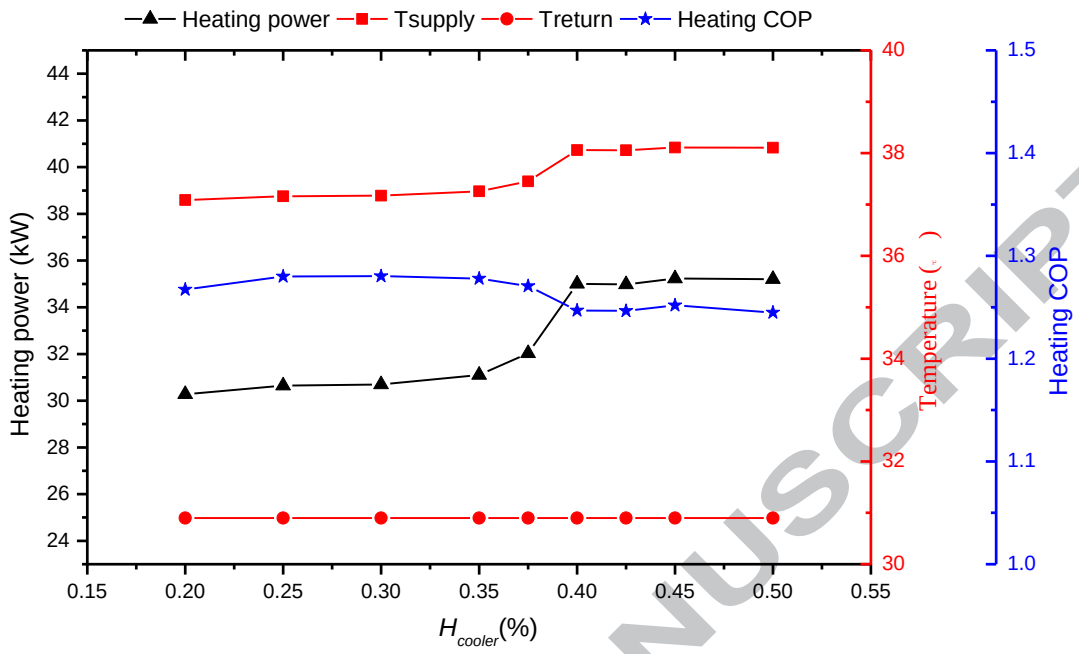

Fig. 10 Effect of H_{cooler} of SSWT on heating performance at 72%_P load

6.1.5 Scenario 5: M_{cond} and M_{cooler} effect on heating performance

The total mass flow (M_{rad}) of cooler and condenser is kept constant according to DIN 4650 in the entire simulation time for all subsequent load cases. M_{rad} is calculated using Eq. (6). In the adsorption half cycle, M_{cond} is zero and M_{cooler} is equal to M_{rad}; in the desorption half cycle, M_{rad} is the total flow at the cooler and condenser side.

$$M_{rad} = P_{design}/(c_p * (T_{supply-design} - T_{return-design})) \quad (6)$$

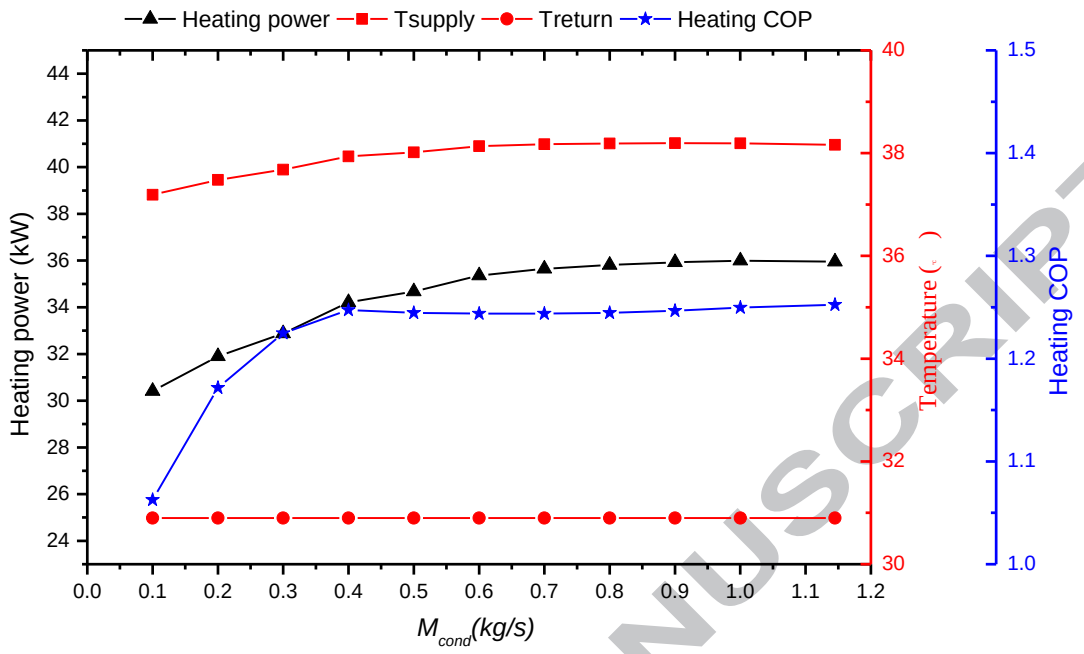

Fig. 11 Effect of M_{cond} of condenser on heating performance at 72%_P load

The effect of M_{cond} of condenser on the heating performance is shown in Fig. 11. It can be observed that increasing M_{cond} will increase the heating power, but the heating COP does not change much when M_{cond} is over 0.4.

6.2 System performance of representative five part load cases

To achieve a higher heating COP and still meet the heating demand for each of the five part loads, we examined the results of these five part loads. As mentioned at Section 6.1, the number of zones, H_{heater}, and H_{cooler} were fixed, whereas M_{sys}, M_{cond}, and T_{diff} were varied with different heating demand cases. Compared to the cases in Section 6.1, the electric heater in Section 6.2 was switched off according to the heater operational schedule (Eq. 4). The main parameter setting for different representative loads is showed in Table 3. The energy performance results of the five part loads for one day are shown in Fig. 12. All the values shown in Fig. 12 are the average for one day. In our simulation control process, we used one and the same chamber as the evaporator and condenser during the adsorption and desorption half cycles (see Fig. 1), respectively. As the same heat exchanger is used alternatingly as an evaporator and condenser, the evaporator has to be cooled at the beginning of the adsorption half-cycle from the medium temperature to the low temperature level. After this cooling-down phase, the evaporator can absorb heat from the ground source. In cases where the heat from the storage is not sufficient for the desorption process, only a small amount of working fluid (water) is evaporated during the adsorption half-cycle. In this case, the amount of heat released to the ground to cool the evaporator is larger than the amount of heat extracted from it for evaporation. Thus, some cycles' heating COPs are lower than 1 at the end of the heater switch off interval in the 72%_P case.

For the 72%_P case, Fig. 12(a) shows that the mean heating power is 34.59 kW and the mean heating COP is 1.16. We can observe that the heating COP decreases drastically after several cycles when the heater is switched off, while the heating power decreases immediately when the heater is switched off. We have three switch off intervals in one day, and every interval lasts for 2 h (see Eq. 4). At the first switch off interval, the heating COP decreases from 1.20 to 0.99 and the heating power decreases from 37.52 kW to 23.91 kW. At the second switch off interval, the heating COP declines to 0.88 because of switching off the heater again after 2 h of recharging. At the last switch off interval, the heating COP decreases from 1.20 to 0.96. We can conclude that a 2 h heater recharging (i.e., 10:00–12:00) is inadequate to recover the storage tank. Although a 4 h heater recharging (i.e., 14:00–18:00) is enough to recover the heating COP, the heating power is not enough, and the heating COPs during all switch off intervals are low. Thus, a 2 h heater switch off is not recommended for high load demands such as over 72%_P case.

For the 61%_P case, Fig. 12(b) shows that the heating power and COP decrease when the heater is switched off. The mean heating power is 31.18 kW, and the mean heating COP is 1.31. We can observe that the heating power decreases from 35.17 kW to 22.24 kW during the heater first switch off interval; meanwhile, the heating COP declines from 1.32 to 1.22, which is acceptable. At the second switch off interval, the heating COP declines from 1.32 to 1.05 and the heating power declines to 18.21 kW, which are unacceptable. At the last interval, the heating power and COP decrease to 18.75 kW and 1.13 respectively, which are still unsatisfactory. We can conclude that the 4 h recharging is not enough to recover the storage tank. The storage tank will be recovered, however, after more than 4 h of recharging (such as 8 h during night recharging). Although the heating COPs are higher than 1 for all cycles and there are fewer cycles being degraded compared to the 72%_P case, the recharging time of less than 4 h between two heater switch off intervals is a poor strategy.

For the 53%_P case, Fig. 12(c) shows that the mean heating power is 27.12 kW and the mean heating COP is 1.37. This figure shows that the heating power slightly falls at the first and last heater switch off intervals. At the second heater switch off interval, the heating power declines from 26.78 kW to 18.15 kW, and heating COP declines from 1.37 to 1.18. Compared to the second interval, the lowest heating COP and heating power at the last interval are significantly improved to 1.26 and 21.4 kW respectively. Thus, the 4 h recharging is enough to recover the storage tank in this case.

To investigate the adsorption process in the adsorber chamber during the heater switch off intervals, the water loading on the adsorbent is shown in Fig. 13. We examine the water loading state of 53%_P case, which includes approximately 13 cycles during the first and second intervals. At the first interval (approximately six cycles), the adsorbate (water) desorbs mostly during the desorption half cycles, which means that the regenerated adsorbent (SAPO-34) has less adsorbate residual after the desorption process. At the 6^{th} cycle of the first switch off interval, the adsorbate mass decreases from 0.29 kg/kg to 0.05 kg/kg, and the heating COP of 1.38 is still higher than the mean value of 1.37. At the second interval (approximately seven cycles), the regenerated adsorbent has an increasing adsorbate residual at the end of each desorption process, which is 0.15 kg/kg at the end of the 7^{th} desorption process. At the second switch off interval, the

adsorbate residual at the end of the desorption half cycle increases from 0.03 kg/kg at the first cycle to 0.15 kg/kg at the 7th cycle. The minimum heating COP is 1.18, which is lower than the mean value of 1.37. This is because the heat is dissipated in the storage tank without heat supply, and an increasing amount of water is accumulated in the adsorbent, which degraded the performance of the adsorption and desorption processes. We found that the storage tank can be recovered after 4 h recharging. Furthermore, Fig. 14 shows the tank temperature of heater switch off intervals for the 53%_P case. Comparing the interval start temperature, we can observe that the tank temperature is considerably degraded at the second interval, while most of its heating capacity is recovered in the last interval. As for the interval end temperature, we can observe even at the second interval that the ending tank temperatures are still higher than 60 °C (60–78 °C) at the heater covered part. Even though this portion of heat cannot be effectively used to drive the adsorber anymore, it could be used as a direct heating supply from the cooler side if the cooler position is adjustable.

In the 44%_P case, the mean heating power is 21.54 kW and the mean heating COP is 1.40. In the 27%_P case, the mean heating power and mean heating COP are 13.96 kW and 1.41 kW respectively. Fig. 12(d) and Fig. 12(e) show that switching off the heater will not degrade the heating COP and heating power practically. In these two cases, the storage tank can be recovered after 2 h recharging so that more electric heater switch off intervals and more than 2 h of each interval can be implemented in real applications without sacrificing the heating COP and heating power significantly. An overview of the results of these five part loads is shown in Fig. 15. All the results are the mean values for the whole simulation day. It can be observed that the heating COP increases when the power load decreases, while the rate of increase in the heating COP slows down when the power load is lower than 44%_P. In Fig. 15, we can observe that the heating COP is nearly the same as those at 44%_P and 27%_P cases.

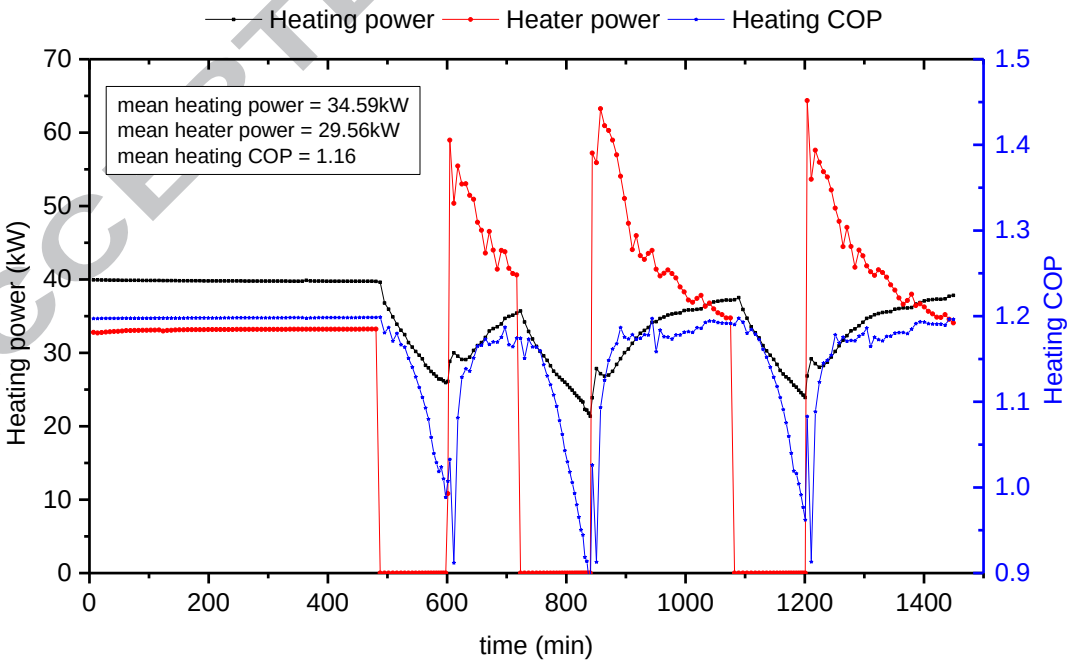

(a) 72%_P case (mass flow = 3.0 kg/s, M_{cond} = 0.6 kg/s, T_{return} = 30.9 ℃, T_{diff} = 5 ℃)

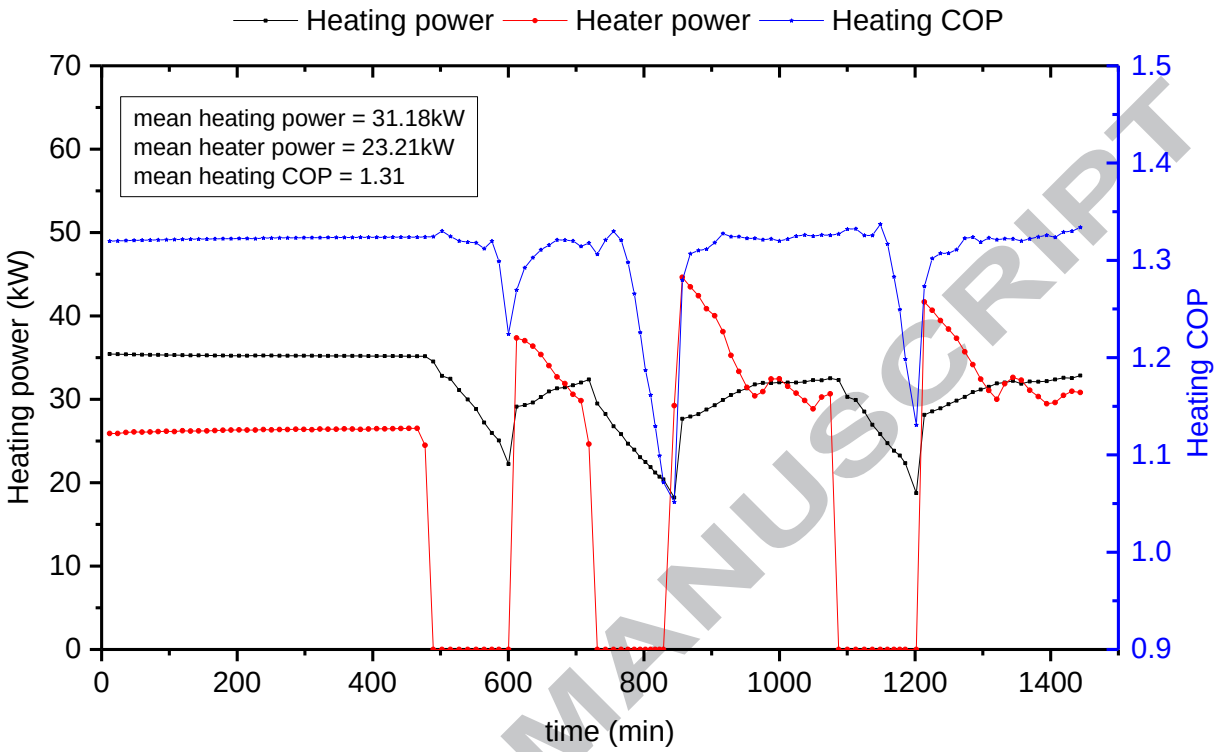

(b) 61%_P case (mass flow = 2.1 kg/s, M_{cond} = 1.145 kg/s, T_{return} = 29.3 ℃, T_{diff} = 5 ℃)

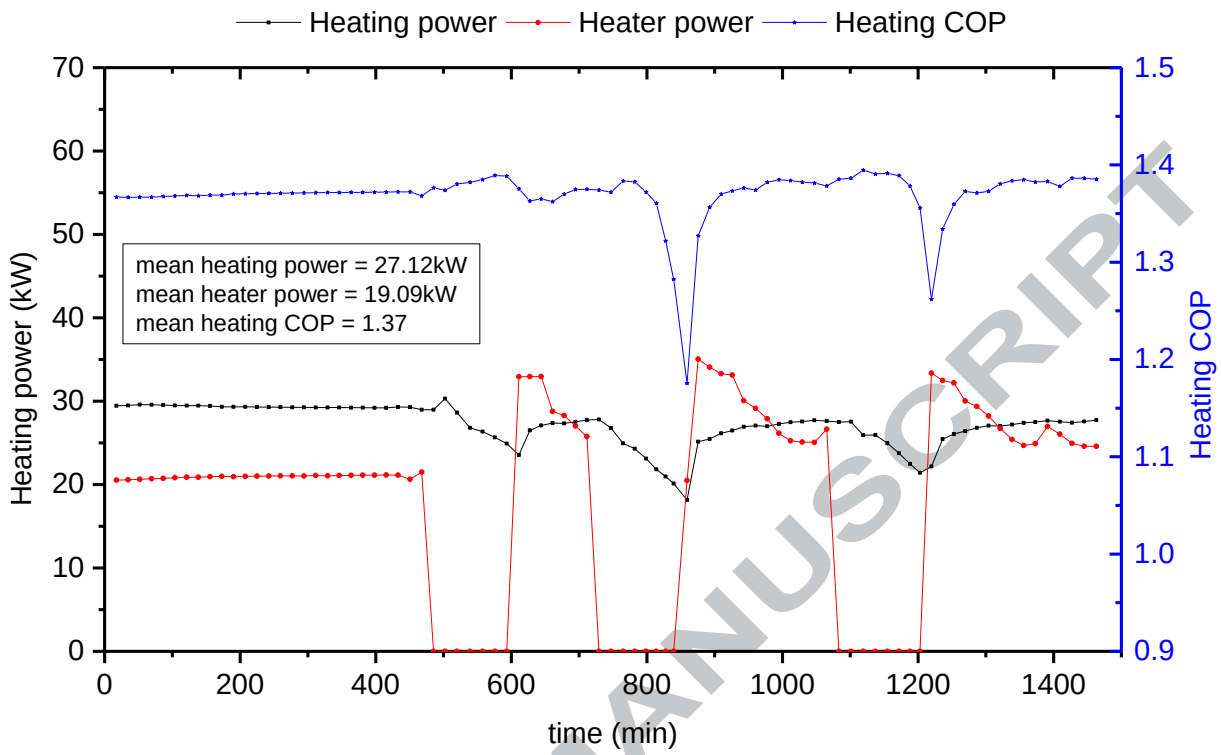

(c) 53%_P case (mass flow = 1.70 kg/s, M_{cond} = 1.145 kg/s, T_{return} = 28.2 ℃, T_{diff} = 4 ℃)

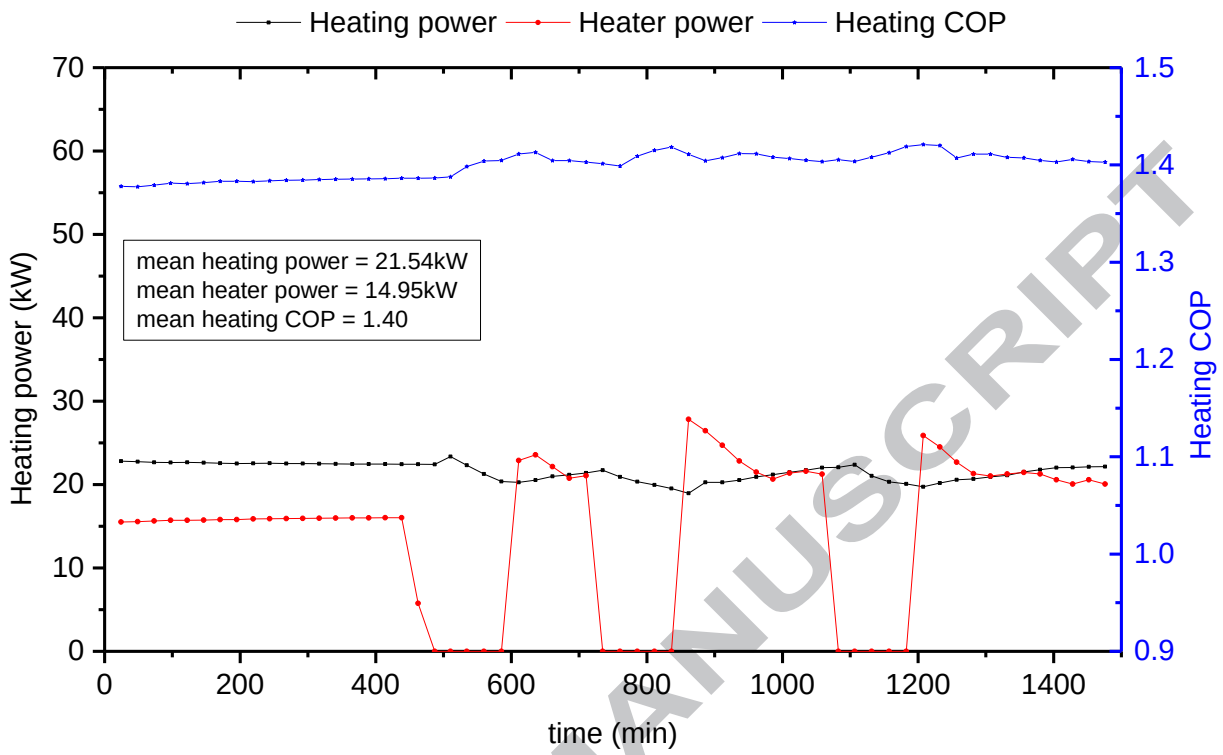

(d) 44%_P case (mass flow = 1.30 kg/s, M_{cond} = 1.145 kg/s, T_{return} = 26.9 ℃, T_{diff} = 4 ℃)

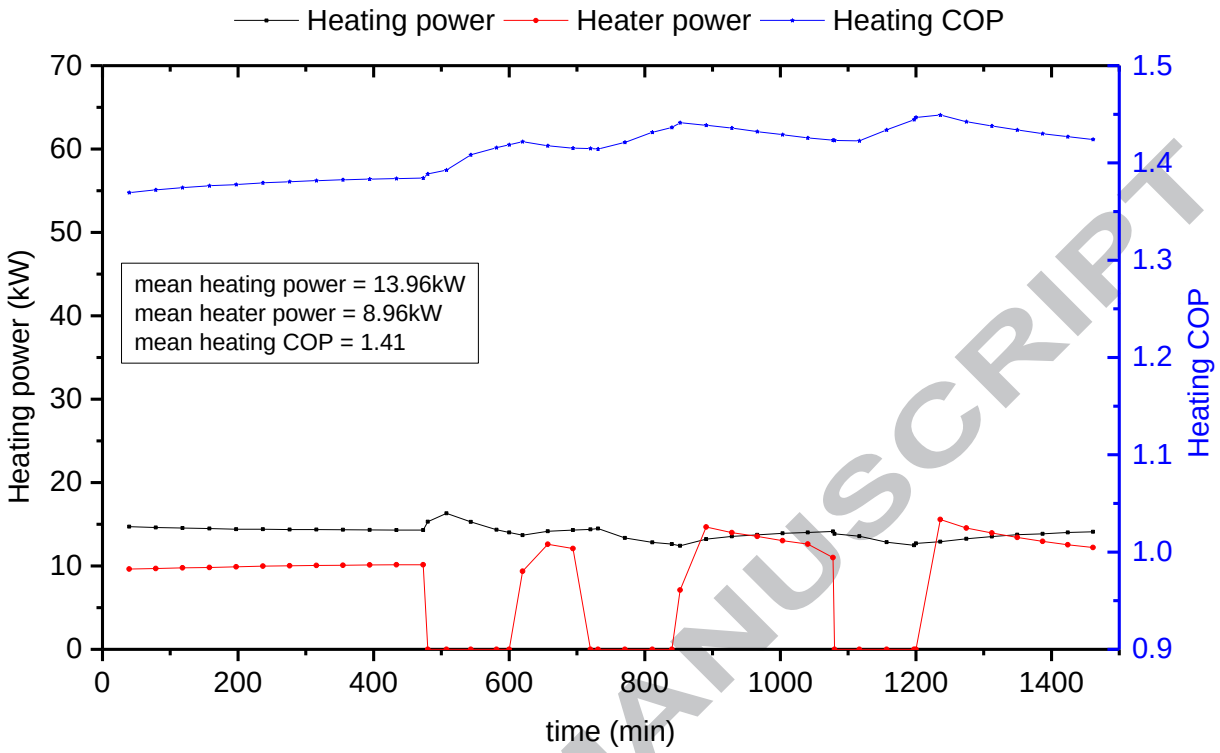

(e) 27%_P case (mass flow = 0.70 kg/s, M_{cond} = 1.145 kg/s, T_{return} = 24.4 °C, T_{diff} = 3 °C)

Fig. 12 Heating COP, heating power, and heater power of representative five part loads

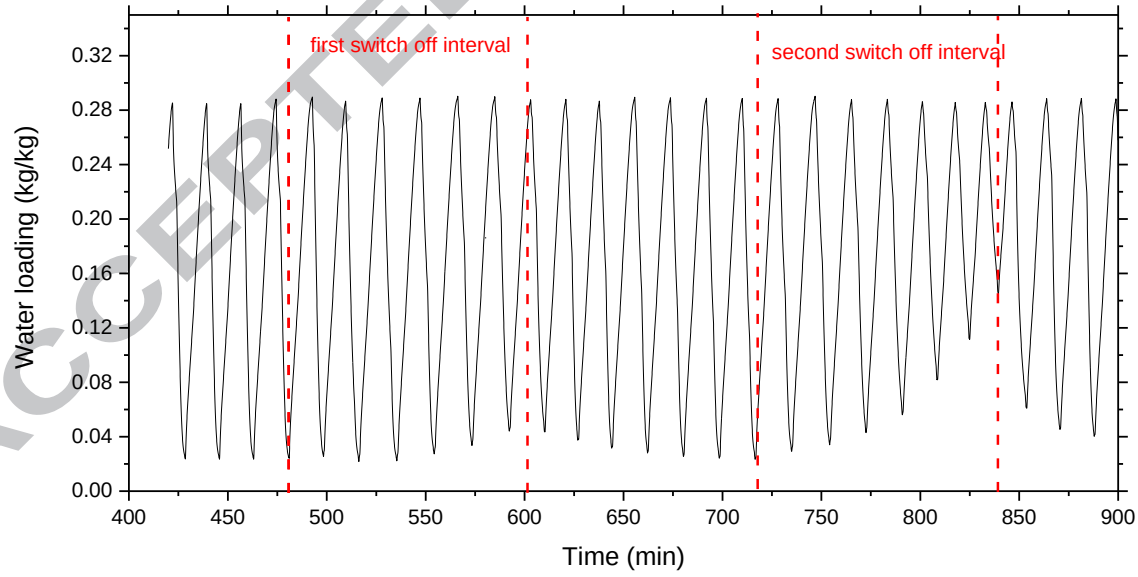

Fig. 13 Water loading of adsorbent during heater switch off intervals (53%_P case)

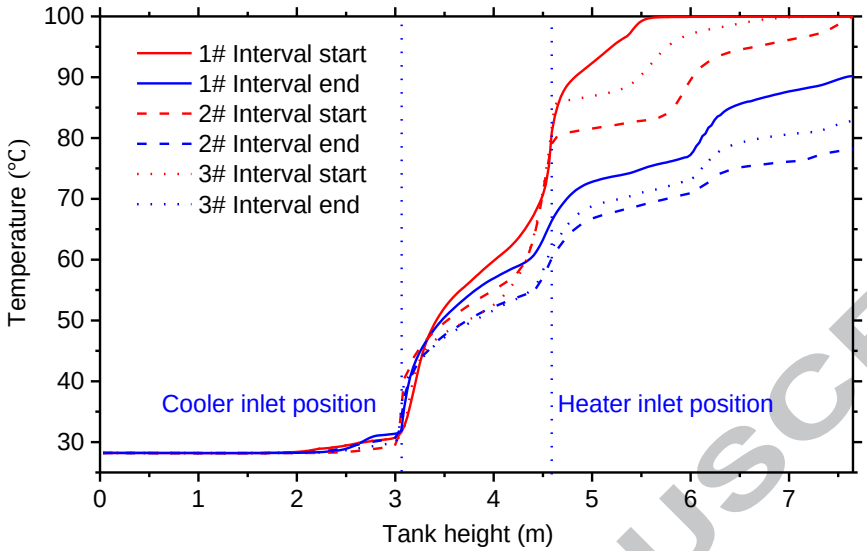

Fig. 14 Storage tank start/end temperature of heater switch off intervals (53%_P case)

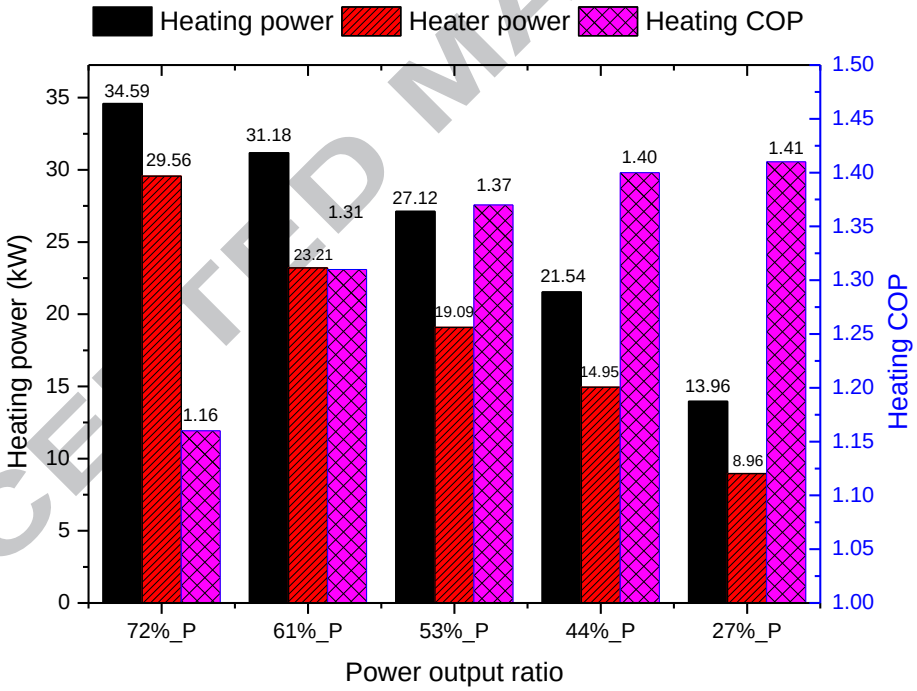

Fig. 15 Overview of the results of the representative five part loads

Table 4 Recommended heater switch off interval and recharging duration of five part loads

Load cases	Switch off interval (2 h)	Recharging duration (2 h)	Recharging duration (4 h)	Recharging duration (8 h)

72%_P	✕	✕	✕	✓
61%_P	✓	✕	✕	✓
53%_P	✓	✕	✓	✓
44%_P	✓	✓	✓	✓
27%_P	✓	✓	✓	✓

Note: ✕ - not recommended, ✓- recommended

In all these cases, the storage tank can be recovered after nighttime recharging. However, a 2 h heater switch off interval is extremely long for high load cases (such as larger than 72%_P), where there is insufficient heat to drive the adsorber without sacrificing the heating efficiency. When the loads are smaller than 61%_P, the switch off interval could be 2 h if the recharging duration is long enough. The recommended heater switch off intervals and recharging duration of each load are listed in Table 4. In real applications, the optimal heater switch off interval and recharging duration can be determined by the real heating demand and electricity price.

6.3 Electricity flexibility

As we know, most of the time the air-conditioning system works at partial design load, while the percentage of actual load and design load is highly related to different buildings. Three-quarters of the design load for real building's flexibility investigation is a reasonable assumption refer to literature review [37, 38]. Therefore, to calculate the electricity flexibility in use of this SAWS system, 72%_P is taken as the case for analysis. Fig. 14 shows the storage tank temperature at some specific times. Usually, as the tank temperature varies between the maximum and minimum temperature, the tank can be charging or discharging through changing the heater power and schedule to provide electricity flexibility anytime. Compared to a reference situation, the electricity consumption increases by increasing the heater power, which denotes a positive flexibility in use according to Eq. (5), and vice versa. The real-time electricity flexibility in use of the SAWS system for the 72%_P case is shown in Fig. 16(a). The area between the actual and maximum heater power is the total positive flexibility potential, and the reference heater power denotes the total negative flexibility potential. It can be observed that the negative flexibility in use reach the maximum when the heater is switched off, and the positive flexibility in use also goes to a high level when the heater is switched on again. In this figure, we can also observe that the available energy flexibility between the actual heater power and the maximum heater power varies over time. It is important to note that if the flexibility potential is used at a specific time, the availability of flexibility at a future time will be changed. Actually, the flexibility potential can be used any time during the day when the heater schedule is changed. Although there is substantial flexibility potential in this system, the flexibility in use is not easy to realize without sacrificing the occupant's thermal comfort. Fig. 16(b) shows the delayed (negative) and forced (positive) energy consumption in one day. The positive and negative flexibilities in use are up to 30.0 kW and −33.0 kW respectively, and the total energy flexibilities

in use are 108 kW and 198 kWh in that case, respectively. Note that the flexibility will be different in other load cases. Generally, there is more energy flexibility in the high power stage and vice versa. With energy flexibility available in buildings, the energy management system, DR programs, and other economic efficiency programs could be more flexible and profitable.

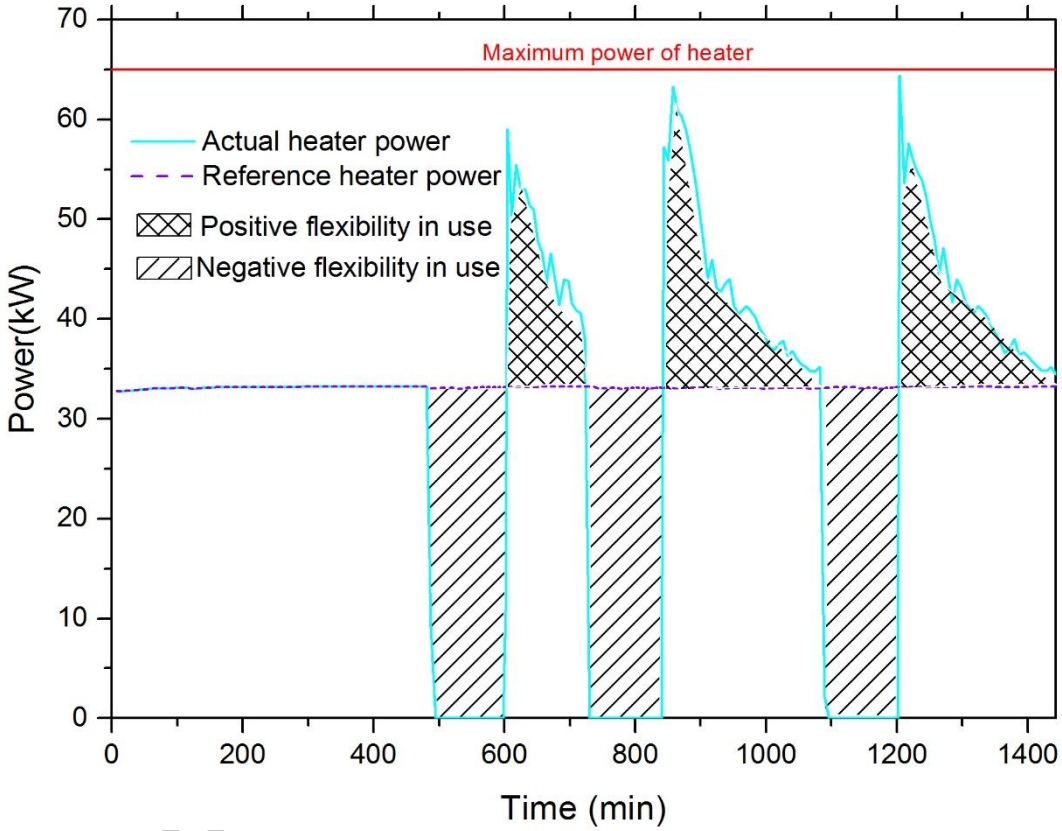

(a) Real-time electricity flexibility in use

(b) Profile of delayed and forced energy flexibility

Fig. 16 Daily flexibility profile of SAWS system for 72%_P case

7 Conclusions

In this study, an innovative AHP with stratified storage tank coupling was investigated. The proposed system works under an electric heater switch off and on schedule that depends on the electricity load and electricity price. Satisfactory energy efficiency and energy flexibility potential were obtained from this system. Several main conclusions are as follows:

(1) The system mass flow has the strongest influence on heating performance. The heating COP decreases drastically and the heating power increases by increasing the system mass flow. Moreover, using more stratified temperature zones is beneficial for improving energy efficiency but increases the complexity and cost of the system.
(2) In our building application, the SAWS system could provide approximately 2 h of adequate heating supply without requiring electricity access. By using the ambient heat from the borehole, this system has a promising heating COP compared to conventional AHP systems.
(3) Although the heating COP is low at the end of some heater switch off intervals, the temperature of the tank is still higher than 60 °C (60–78 °C) at the electric heater covered part, and only approximately half of the storage volume is available as heat buffer volume in this study. There is still plenty of heat for direct heating by extracting heat from the cooler side if the cooler position is changeable (e.g., by installing multiport valves) in a real system, and the storage density efficiency will be higher.
(4) The SAWS system can provide energy flexibility almost anytime, and the maximum positive and negative electricity flexibilities are up to 30 kW and −33 kW in the 72%_P case. The flexibility potential will vary with different load cases. This system is promising for DR programs and energy management systems owing to its relatively high energy flexibility potential and energy efficiency for buildings in heating-dominated regions.

Acknowledgments:

We acknowledge the funding by the German Federal Ministry for Economic Affairs and Energy in the framework of the LowEx-Bestand project (grant number 03SBE0001A). We thank Mr. Martin Kleinstück (Fraunhofer ISE) for providing the heating load series of the reference building.

Appendix Table 1

Detailed parameter setting in SAWS simulation system

 # System parameters

- System mass flow M_{sys} = variable
- Number of fluid nodes in adsorber = 16
- Number of pipes nodes = 12

 # Evaporator and condenser specification

- Overall heat transfer conductivity of condenser = 400 (W/(m^2·K))
- Heat exchanger area of condenser = 25 m^2
- Mass flow in condenser M_{cond} = variable
- Mass of copper in condenser = 23 kg
- Overall heat transfer conductivity of evaporator = 400 (W/(m^2·K))
- Heat exchanger area of evaporator = 25 m^2
- Mass flow in evaporator = 2.22 kg/s
- Mass of water in adsorber chamber = 5 kg
- Mass of copper in evaporator = 23 kg

 # Electric heater and cooler parameters

- Mass flow of cooler M_{cooler} = variable
- Maximum heater power = 65 kW
- Electric heater position H_{heater} = variable
- Cooler position H_{cooler} = variable

 # Adsorber parameters

- Mass of adsorbent = 16.45 kg
- Adsorbate = water
- Adsorbent = SAPO-34

 # Temperature setting

- Maximal regeneration temperature = 100 °C
- Evaporator temperature = 9.54 °C
- Condenser temperature T_{return} = variable

 # Heat exchanger

- Heat exchanger type = ideal
- Cooler type = ideal

 # Storage parameters

- Water mass in storage = 2250 kg
- Number of zones for water extraction = variable

References:

[1] Rubin ES, Azevedo IML, Jaramillo P, Yeh S. A review of learning rates for electricity supply technologies. Energ Policy. 2015;86:198-218.

[2] Criqui P, Mima S, Menanteau P, Kitous A. Mitigation strategies and energy technology learning: An assessment with the POLES model. Technological Forecasting and Social Change. 2015;90:119-36.

[3] Luo G, Dan E, Zhang X, Guo Y. Why the Wind Curtailment of Northwest China Remains High. Sustainability-Basel. 2018;2(10):570.

[4] Joos M, Staffell I. Short-term integration costs of variable renewable energy: Wind curtailment and balancing in Britain and Germany. Renewable and Sustainable Energy Reviews. 2018;86:45-65.

[5] Mark K, Martin B, Klaus P. Possible role of power-to-heat and power-to-gas as flexible loads in German medium voltage networks. Front. Energy. 2017;2(11):135-45.

[6] Weitemeyer S, Kleinhans D, Vogt T, Agert C. Integration of Renewable Energy Sources in future power systems: The role of storage. Renew Energ. 2015;75:14-20.

[7] Arteconi A, Hewitt NJ, Polonara F. Domestic demand-side management (DSM): Role of heat pumps and thermal energy storage (TES) systems. Appl Therm Eng. 2013;51(1-2):155-65.

[8] Palzer A, Henning H. A comprehensive model for the German electricity and heat sector in a future energy system with a dominant contribution from renewable energy technologies – Part II: Results. Renewable and Sustainable Energy Reviews. 2014;30:1019-34.

[9] Hedegaard K, Mathiesen BV, Lund H, Heiselberg P. Wind power integration using individual heat pumps – Analysis of different heat storage options. Energy. 2012;47(1):284-93.

[10] Hedegaard K, Münster M. Influence of individual heat pumps on wind power integration – Energy system investments and operation. Energ Convers Manage. 2013;75:673-84.

[11] Reynders G, Lopes RA, Marszal-Pomianowska A, Aelenei D, Martins J, Saelens D. Energy flexible buildings: An evaluation of definitions and quantification methodologies applied to thermal storage. Energ Buildings. 2018;166:372-90.

[12] Allison J, Bell K, Clarke J, Cowie A, Elsayed A, Flett G, et al. Assessing domestic heat storage requirements for energy flexibility over varying timescales. Appl Therm Eng. 2018;136:602-16.

[13] Fischer D, Madani H. On heat pumps in smart grids: A review. Renewable and Sustainable Energy Reviews. 2017;70:342-57.

[14] Lehmann C, Beckert S, Glaeser R, Kolditz O, Nagel T. Assessment of adsorbate density models for numerical simulations of zeolite-based heat storage applications. Appl Energ. 2017;185(SI2):1965-70.

[15] Henninger SK, Schmidt FP, Henning HM. Water adsorption characteristics of novel materials for heat transformation applications. Appl Therm Eng. 2010;30(13):1692-702.

[16] Henninger SK, Ernst S, Gordeeva L, Bendix P, Fröhlich D, Grekova AD, et al. New materials for adsorption heat transformation and storage. Renew Energ. 2017;110:59-68.

[17] Bonaccorsi L, Bruzzaniti P, Calabrese L, Freni A, Proverbio E, Restuccia G. Synthesis of SAPO-34 on graphite foams for adsorber heat exchangers. Appl Therm Eng. 2013;61(2):848-52.

[18] Rivero-Pacho AM, Critoph RE, Metcalf SJ. Modelling and development of a generator for a domestic gas-fired carbon-ammonia adsorption heat pump. Renew Energ. 2017;110:180-5.

[19] Freni A, Dawoud B, Bonaccorsi L, Chmielewski S, Frazzica A, Calabrese L, et al. Characterization of Zeolite-Based Coatings for Adsorption Heat Pumps.: Springer International Publishing, 2015.

[20] Calabrese L, Brancato V, Bonaccorsi L, Frazzica A, Capri A, Freni A, et al. Development and characterization of silane-zeolite adsorbent coatings for adsorption heat pump applications. Appl Therm Eng. 2017;116:364-71.

[21] Bauer J, Herrmann R, Mittelbach W, Schwieger W. Zeolite/aluminum composite adsorbents for application in adsorption refrigeration. Int J Energ Res;33(13):1233-49.

[22] Wittstadt U, Füldner G, Andersen O, Herrmann R, Schmidt F. A New Adsorbent Composite Material Based on Metal Fiber Technology and Its Application in Adsorption Heat Exchangers. Energies. 2015;8(8):8431-46.

[23] Wittstadt U, Füldner G, Laurenz E, Warlo A, Große A, Herrmann R, et al. A novel adsorption module with fiber heat exchangers: Performance analysis based on driving temperature differences. Renew Energ. 2017;110:154-61.

[24] Chen Y, Xu P, Gu J, Schmidt F, Li W. Measures to improve energy demand flexibility in buildings for demand response (DR): A review. Energ Buildings. 2018;177:125-39.

[25] Björn F, Christoph W. The value(s) of flexible heat pumps – Assessment of technical and economic conditions. Appl Energ. 2018;228:1292-319.
[26] Kirkerud JG, Bolkesjo TF, Tromborg E. Power-to-heat as a flexibility measure for integration of renewable energy. Energy. 2017;128:776-84.
[27] Hussain A, Bui V, Kim H, Im Y, Lee J. Optimal Energy Management of Combined Cooling, Heat and Power in Different Demand Type Buildings Considering Seasonal Demand Variations. Energies. 2017;10(7896).
[28] Schwamberger V, Schmidt F. Smart use of a stratified hot water storage through the coupling to an adsorption heat pump cycle, in Proceedings of 8th International Renewable Energy Storage Conference and Exhibition, Berlin, Germany, 2013.
[29] Li W, Chen Y, Xu P, Joshi C, Schmidt F. Research on the performance of an adsorption heat pump in winter demand response. Sci Technol Built En. 2017(23):449-56.
[30] Schwamberger V, Joshi C, Schmidt F. Second law analysis of a novel cycle concept for adsorption heat pumps, in Proceedings of International Sorption Heat Pump Conference, Padua, Italy, 2011.
[31] Joshi C. Experimental Investigations of Adsorption Chiller Cycle Using Stratified Thermal Storage for Heat Recovery: Karlsruher Institut für Technologie (KIT), 2016.
[32] Treier MS, Desai A, Schmidt FP. Comparison of storage density and efficiency for cascading adsorption heat storage and sorption assisted water storage, in Proceedings of the 8th Heat Powered Cycles Conference, Bayreuth, Germany, 2018.
[33] Ulbig A, Andersson GR. Analyzing operational flexibility of electric power systems. Int J Elec Power. 2015;72:155-64.
[34] Chen Y, Xu P, Gu J, Schmidt F, Li W. Measures to improve energy demand flexibility in buildings for demand response (DR): A review. Energ Buildings. 2018;177:125-39.
[35] Schwamberger V. Thermodynamische und numerische Untersuchung eines neuartigen Sorptionszyklus zur Anwendung in Adsorptionswärmepumpen und -kältemaschinen: Karlsruher Institut für Technologie (KIT), 2016.
[36] Bauer J, Herrmann R, Mittelbach W, Schwieger W. Zeolite/aluminum composite adsorbents for application in adsorption refrigeration. International Journal of Energy. 2009(33):1233-49.
[37] Hong TZ, Chou SK, Bong TY. A design day for building load and energy estimation. Build Environ. 1999;34(4):469-77.
[38] Escriva-Escriva G, Alvarez-Bel C, Valencia-Salazar I. Method for modelling space conditioning aggregated daily load curves: Application to a university building. Energ Buildings. 2010;42(8):1275-82.

Highlights

1. Energy performance and energy flexibility of a novel system were investigated.
2. An average heating COP of 1.33 is achieved for five representative load cases.
3. This system achieves considerable electricity flexibility for a residential building.
4. This novel system can provide 2 hours of heating supply without electricity access.